Journal of Alloys and Compounds, 189 (1992) 209–215
JALCOM 383

Metal sulphide–tetraphosphorusdekasulphide phase diagrams

Heike Andrae and Roger Blachnik
Anorganische Chemie, Universität Osnabrück, Barbarastraße 7, W-4500 Osnabrück (Germany)

(Received May 25, 1992)

Abstract

The phase diagrams of the quasibinary systems Ag_2S–P_4S_{10}, Cu_2S–P_4S_{10}, Tl_2S–P_4S_{10} and Sb_2S_3–P_4S_{10} were determined by means of difference thermal and X-ray analyses. Ag_2S–P_4S_{10} contains the congruently melting compound Ag_7PS_6, the peritectic compounds Ag_3PS_4, $Ag_4P_2S_7$ and $Ag_2P_2S_6$ and the peritectoid high temperature compound $Ag_7P_3S_{11}$. The lattice parameters of Ag_3PS_4 and of a new high temperature modification of $Ag_4P_2S_7$ were determined: Ag_3PS_4, space group $Pmn2_1$, $a=765.0(1)$, $b=686.8(1)$, $c=650.9(1)$ pm; HT-$Ag_4P_2S_7$, $a=807.3(2)$, $b=1102.2(3)$, $c=636.8(2)$ pm, $\beta=105.22(3)°$. In the system Cu_2S–P_4S_{10} the congruently melting compound Cu_7PS_6, the peritectic compound Cu_3PS_4 and the new metathiophosphate $(CuPS_3)_n$ were observed. The IR and Raman spectra of the compounds are given. The systems Tl_2S–P_4S_{10} and Sb_2S_3–P_4S_{10} are simple. Similar to the system Ag_2S–P_4S_{10}, miscibility gaps were found on the P_4S_{10}-rich side of these systems. The compounds Tl_3PS_4, $Tl_2P_2S_6$ and $SbPS_4$ (lattice parameters $a=1306.03(5)$, $c=627.9(5)$ pm) melt congruently.

1. Introduction

Materials with non-linear optical properties have found growing interest in materials science research groups. Until now, the investigations have mainly dealt with oxide-based systems. One condition for non-linear optical effects is the absence of a centre of inversion, *i.e.* that the compound crystallizes in an acentric space group. The average percentage of such compounds in inorganic compounds is 15%. This probability becomes larger in materials such as sulphides and oxocompounds of phosphorus [1]. The increased occurrence of acentric structures in these systems is possibly related to the polarizability of the S^{2-} and PS_4^{3-} building units. The latter groups can be linked to various structural motifs which give rise to numerous compounds. Some of these must crystallize in acentric space groups. For this reason we are investigating the phase relations in ternary metal–phosphorus–sulphur systems. In this paper we report the quasibinary cross-sections Cu_2S–P_4S_{10}, Ag_2S–P_4S_{10}, Tl_2S–P_4S_{10} and Sb_2S_3–P_4S_{10}.

2. Experimental details

High purity elements (copper 99.999%, silver 99.999%, Degussa; thallium 99.999%, Ventron; antimony 99.999%, Preussag; phosphorus, ultrapure, electronic grade, Hoechst AG, Werk Knapsack; sulphur, chem. pure, cryst., Riedel de Haen AG) were mixed in stoichiometric amounts for preparation of the binary compounds which form the systems. The preparation was carried out in evacuated quartz ampoules which were first heated above the melting points of the elements and then annealed slightly below the melting point of the compounds. The purity of the products was confirmed by X-ray analysis. For investigation of the systems, mixtures were made in steps of 5 mol% from these compounds and transferred into quartz ampoules. These were evacuated and sealed. The reactants were first melted in a flame and shaken vigorously to homogenize the melt. The samples were then annealed in the solid state for periods between two weeks and two months and afterwards quenched to ambient temperature. Samples of each product were ground to a powder and transferred into thin-walled tubes of 2–3 mm outer diameter, which were then evacuated and sealed. A previously described apparatus [2] was used for the differential thermal analysis (DTA) measurements of these samples. The thermograms were recorded with silicon as reference material. The heating and cooling rates were 10 K min^{-1}. Other samples were investigated by X-ray methods (Guinier-4 (Huber), automated diffractometer system (Stoe), Guinier-Simon FR 533 (Enraf Nonius), all with Cu Kα radiation). X-ray data were evaluated by the program LSUCR [3]. These DTA- and X-ray data were used to construct the phase diagrams of the systems.

IR and Fourier IR spectra (650–35 cm^{-1}) were obtained at 300 K with a spectrometer IFS-114 (Bruker),

0925-8388/92/$5.00

the powdered samples being dispersed in Nujol or CsI. The Raman spectra were recorded using an Omar-89 (Dilor), fitted with a krypton laser.

3. Results

Although the systems Cu_2S–P_4S_{10} and Ag_2S–P_4S_{10} reveal some differences, both show essentially similar features because the metal ions in these systems, Figs. 1 and 2, have the d^{10} configuration. The liquidi of both are determined by the high-melting $Cu(Ag)_7PS_6$ compound. From the melting points of these mainly metallic sulphides the liquidi descend steeply to degenerated eutectica with eutectic temperatures, which are close to the melting point of molecular P_4S_{10}. Both systems contain a number of compounds which are listed in Table 1. One important difference between these systems is a miscibility gap in the liquid state which was only observed in the Ag_2S–P_4S_{10} system. A second variation is disclosed in the concentration region between the compounds M_3PS_4 and MPS_3. In this part two additional compounds are found in the silver sulphide system.

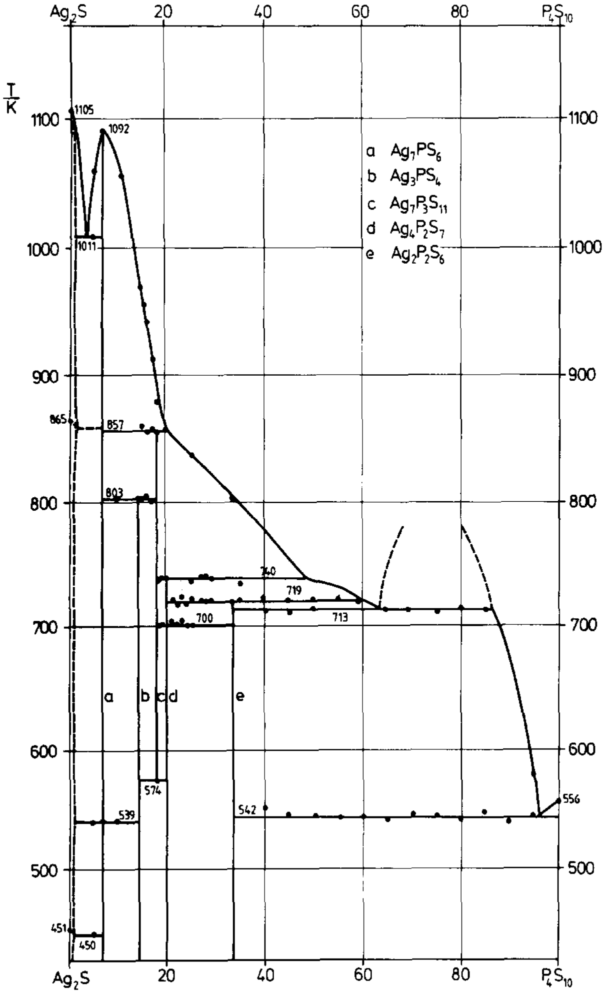

Fig. 1. The system Ag_2S–P_4S_{10}.

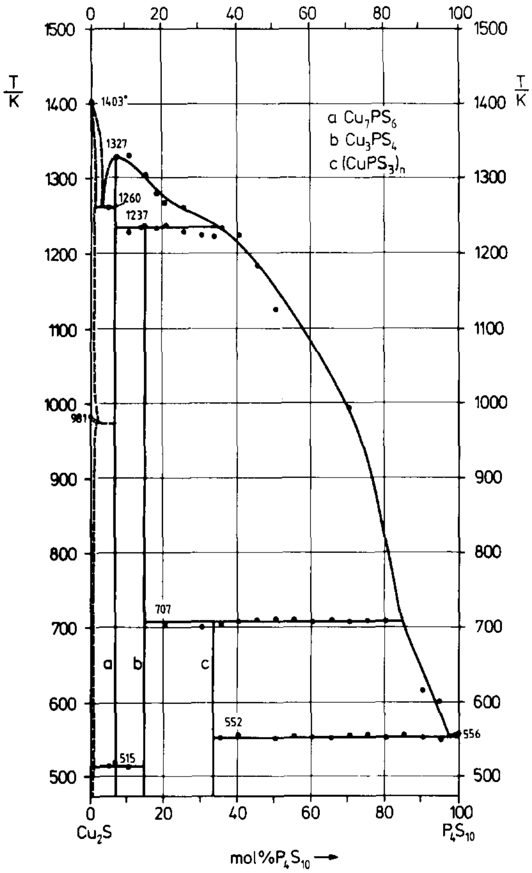

Fig. 2. The system Cu_2S–P_4S_{10}.

The structure of P_4S_{10} is based on a tetrahedral arrangement of atoms, in which the phosphorus atoms are surrounded by four sulphur atoms. The decasulphide can undergo nucleophilic attack, which can lead to compounds with discrete tetrahedral PS_4^{3-} anions or to dimers, in which these tetrahedra are linked together by sharing one or two sulphur atoms. By the addition of M_2S the molecule P_4S_{10} will disintegrate similarly by rupture of P–S–P bridges by the attack of excess sulphur ions.

The PS_4^{3-} tetrahedra will occur isolated or connected to oligomers via common corners or edges in the structures of the compounds depending on the S^{2-} ion concentration. Cu_7PS_6 [4] and Ag_7PS_6 [7] formed with the highest excess of S^{2-}, are both members of the argyrodite family. In a simplified description one may consider the structure as an Ag_2S matrix containing isolated PS_4^{3-} ions. In their high-temperature modifications a disordered metal(I) ion substructure is found. It shows good ionic conductivity owing to the high mobility of the monovalent cations. On cooling an ordered phase is formed. Tetrahedra are also found in Cu_3PS_4 and Ag_3PS_4 by spectroscopic measurements. The structure of Ag_3PS_4 has not yet been determined.

TABLE 1. Compounds of the systems Cu_2S–P_4S_{10} and Ag_2S–P_4S_{10}

Compound	Type	T_u	T_{per}[a] (K)	T_m (K)	Space group	Lattice parameters (pm)	Reference
Cu_7PS_6 (LT)		515 508			$P2_13$	$a=967.09(6)$ $a=967.3(1)$	 4
Cu_7PS_6 (HT)	Congruent			1327 1318	$F\bar{4}3m$	$a=971.3(2)$, $T=587$ K $a=971(2)$, $T=508$ K	4
Cu_3PS_4	Peritectic		1237		$Pmn2_1$	$a=729.67(6)$, $b=632.65(4)$, $c=607.22(8)^b$ $a=729.6(2)$, $b=631.9(2)$, $c=607.2(2)^b$ $a=643$, $b=755$, $c=612$	 5 6
$(CuPS_3)_n$	Peritectic		707		?		
Ag_7PS_6 (LT)		539 495			$P2_13$	$a=1039.44(9)$ $a=1040.2(2)$	 7
Ag_7PS_6 (HT)	Congruent			1092 1065	$F\bar{4}3m$	$a=1050.2(2)$, $T=560$ K $a=1048.6(5)$, $T=573$ K	 8
Ag_3PS_4	Peritectoid		803		$Pmn2_1$	$a=765.0(1)$, $b=686.8(1)$, $c=650.9(1)$	
$Ag_7P_3S_{11}$	Peritectic		857		$B2/b$	$a=2397.1(5)$, $b=2489.9(6)$, $c=635.4(2)$, $\gamma=110.96(2)°$ $a=2397(1)$, $b=2488(1)$, $c=636.1(4)$, $\gamma=110.85(5)^{\circ b}$	 9
$Ag_4P_2S_7$ (LT)		700			$B2/b$	$a=1078.8(2)$, $b=1621.1(4)$, $c=653.8(1)$, $\gamma=106.8(2)°$ $a=1077.8(5)$, $b=1621.1(8)$, $c=653.4(3)$, $\gamma=106.8(1)^{\circ b}$	 10
$Ag_4P_2S_7$ (HT)	Peritectic		740		Monoclinic (A-centred)	$a=807.3(2)$, $b=1102.2(3)$, $c=636.8(2)$, $\beta=105.22(3)°$	
$Ag_2P_2S_6$	Peritectic		719		$B2/m$	$a=1123.8(1)$, $b=674.2(2)$, $c=701.8(2)$, $\gamma=126.96(2)$ $a=1121.0(3)$, $b=673.1(2)$, $c=699.8(2)$, $\gamma=126.84(2)^b$	 11

[a] No literature data are given for this temperature, because the peritectic character of these compounds was not recognized in former works.

[b] Single-crystal data; LT low temperature modification, HT high temperature modification.

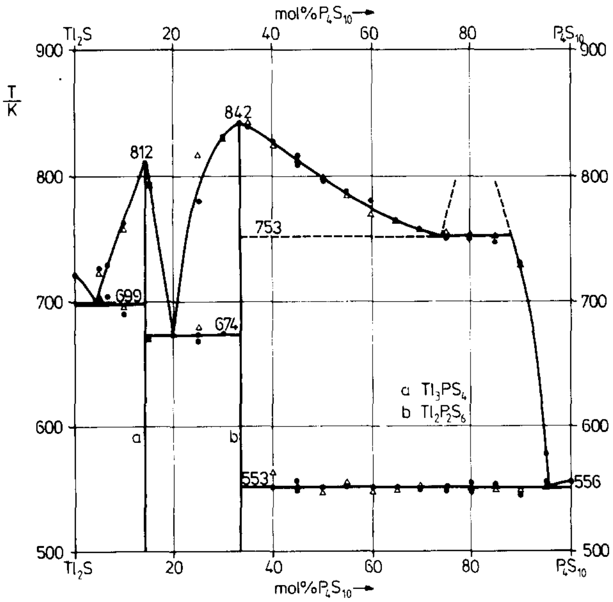

Fig. 3. The system Tl_2S–P_4S_{10} (annealing temperatures △ 403 K, ○ 513 K).

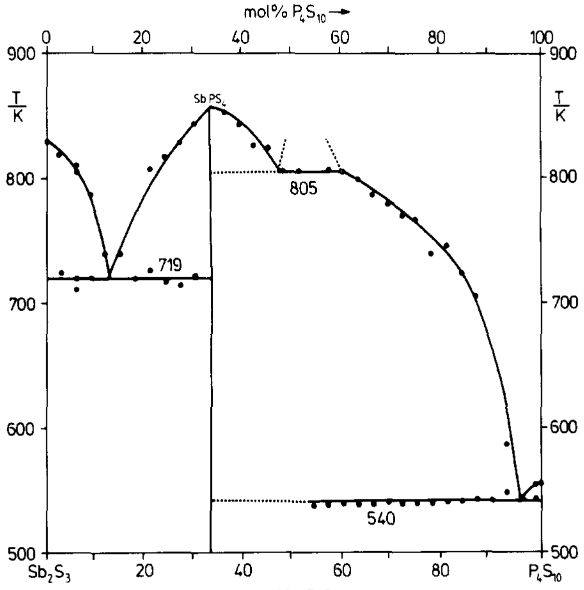

Fig. 4. The system Sb_2S_3–P_4S_{10}.

From the similarity of the vibration spectra Pätzmann and Brockner [12] concluded that Ag_3PS_4 should crystallize in the enargite structure [13]. We simulated the X-ray pattern of Ag_3PS_4 (Table 2) with the aid of the program Lazy Pulverix [14] and the atomic positions of Cu_3PS_4 [5]. A good agreement between simulated

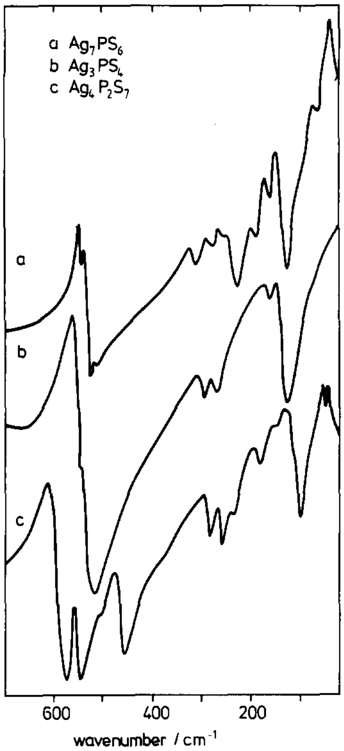

Fig. 5. Fourier IR spectra of Ag_7PS_6, Ag_3PS_4 and $Ag_4P_2S_7$.

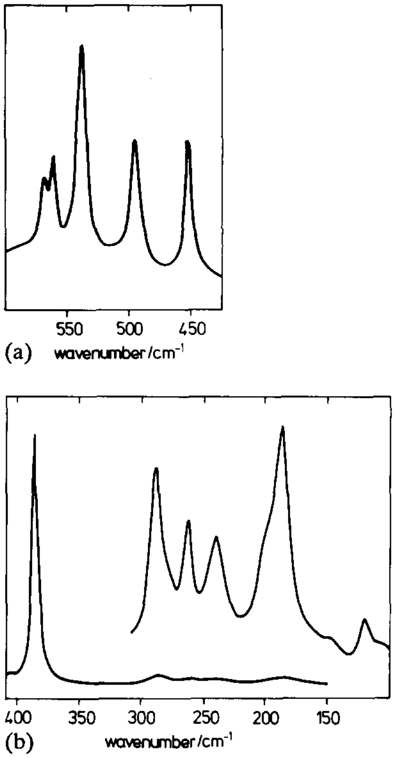

Fig. 7. Raman spectrum of $Ag_4P_2S_7$: (a) 600–425 cm^{-1} relative intensity 300, (b) 400–100 cm^{-1} relative intensity 900.

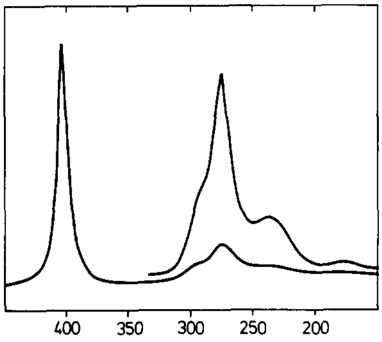

Fig. 6. Raman spectrum of Ag_3PS_4.

and experimental X-ray reflections was obtained, indicating that Ag_3PS_4 crystallizes in the enargite structure. In the $P_2S_7^{4-}$ unit which was observed in $Ag_4P_2S_7$ [10], and together with isolated PS_4^{3-} groups in $Ag_7P_3S_{11}$ [9], two tetrahedra share a corner. $Ag_4P_2S_7$ exists in two modifications, of which the structure of the low temperature form was reported by Toffoli *et al.* [10]. This phase transforms at 700 K into a high temperature form with monoclinic symmetry (Table 3). Surprisingly, $Cu_4P_2S_7$, (cubic, $a = 1034(4)$) pm, could not be prepared in annealing experiments at temperatures between 600 and 1000 K, though it had been reported in the literature [15]. In the metathiophosphate $Ag_2P_2S_6$ [11] two PS_4^{3-} tetrahedra are connected by a common edge. We also observed a metathiophosphate in the copper system, but were not able to prepare single crystals of $(CuPS_3)_n$, therefore no structural information can be given. However, the compound should contain edge-sharing tetrahedra. Its X-ray data are given in Table 4.

Additionally, two phase diagrams Tl_2S–P_4S_{10} and Sb_2S_3–P_4S_{10} were investigated, in which the metal ions have an s^2-electron configuration. Samples of the system Tl_2S–P_4S_{10} were annealed at 403 and 513 K. The phase diagram is given in Fig. 3. The system has a eutectic at 699 K and approximately 4 mol% P_4S_{10}. The compound Tl_3PS_4 [16] melts congruently at 812 K. A second eutectic equilibrium is found between Tl_3PS_4 and $Tl_2P_2S_6$. The eutectic composition and temperature are approximately 20 mol% P_4S_{10} and 674 K respectively. $Tl_2P_2S_6$ [17] melts congruently at 842 K. The region between 33 mol% P_4S_{10} and P_4S_{10} is determined by a third eutectic and a monotectic equilibrium with temperatures of 753 and 553 K. No solid solubility in either of the constituent components was observed. A recent investigation of Tl_3PS_4 shows a width of the homogeneity region of 3.2 mol% P_4S_{10} at 298 K [18]. As expected, the structure of Tl_3PS_4 contains isolated PS_4^{3-} tetrahedra and that of $Tl_2P_2S_6$ contains corner-sharing tetrahedra [16, 17]. The section Tl_2S–"P_4S_6" is not quasibinary. In samples annealed at 513 K we observed $Tl_2S + Tl_3PS_4$ between 0 and 20 mol%, the compounds Tl_3PS_4 and

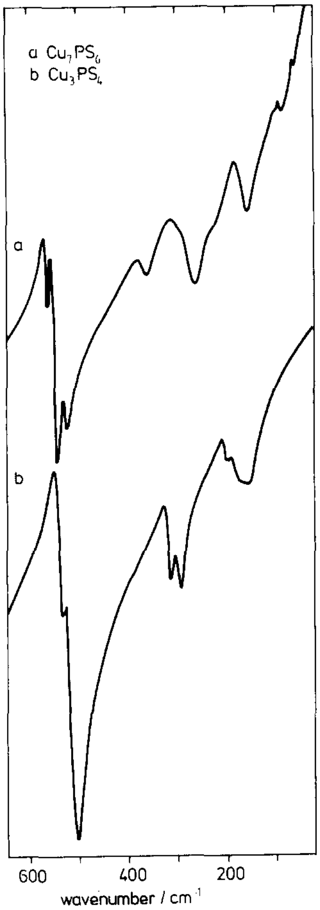

Fig. 8. Fourier IR spectra of Cu_7PS_6 and Cu_3PS_4.

$TlPS_2$ in the small concentration range between 20 and 25 mol%, only $TlPS_2$ between 25 and 36 mol%, and $TlPS_2$ and $Tl_2P_2S_6$ between 36 and 50 mol% "P_4S_6".

The system Sb_2S_3–P_4S_{10} (Fig. 4) was constructed on the basis of data obtained from samples annealed at 600 and 500 K respectively and contains two eutectic and one monotectic equilibria and the congruently melting compound $SbPS_4$. The eutectic equilibria were observed at 719 K, 12.8 mol% P_4S_{10} and 540 K, 95.5 mol% P_4S_{10}. A miscibility gap appears between approximately 55 and 65 mol% P_4S_{10}, which has a monotectic temperature of 805 K. The homogeneity range of $SbPS_4$ extends at 540 K from the stoichiometric composition to 50 mol% P_4S_{10}. The recently reported wide solid solution region based on Sb_2S_3 with a limiting Sb_2S_3–P_2S_5 ratio of 6:1 and the compound SbP_3S_9 [19] were not found in our experiments. The relevant data of the compounds are presented in Table 5. The habit of the $SbPS_4$ crystal (yellow hair-like crystals) allows the conclusion that in this compound PS_4^{3-} tetrahedra are linked in chains. A preliminary investigation of SnS–P_4S_{10} revealed the non-quasibinary character of the system.

The IR and Raman spectra of Ag_3PS_4 [12], $Ag_4P_2S_7$ [20], $Ag_2P_2S_6$ [20] and Cu_3PS_4 [12, 21, 22] have been reported. In order to characterize the thiophosphates completely, we give the spectra of those compounds, for which literature data are not available or contain spectral lines due to impurities. The Fourier IR and Raman spectra of Ag_7PS_6, Ag_3PS_4 and low temperature $Ag_4P_2S_7$ are given in Figs. 5–7. The Fourier IR spectra of Cu_7PS_6 and Cu_3PS_4 are depicted in Fig. 8.

The orthothiophosphates and the argyrodites in the investigated systems crystallize in acentric space groups. Determinations of their electro-optical properties are in progress.

TABLE 2. X-ray-powder data of Ag_3PS_4

$2\theta_{exp}$[a] (deg)	d_{exp} (pm)	$h\ k\ l$	I/I_0	$\Delta 2\theta$[b] (deg)	$2\theta_{exp}$[a] (deg)	d_{exp} (pm)	$h\ k\ l$	I/I_0	$\Delta 2\theta$[b] (deg)
17.363	510.31	1 1 0	8.9	−0.026	43.470	208.01	1 3 1	5.9	0.037
17.840	496.78	1 0 1	3.8	0.039	43.712	206.91	0 1 3	11.6	0.009
18.781	472.09	0 1 1	13.4	−0.013	45.044	201.10	2 2 2	7.6	0.029
22.113	401.65	1 1 1	9.5	−0.017	46.189	196.38	2 3 0	19.5	−0.015
25.937	343.24	0 2 0	32.7	−0.013	47.510	191.22	4 0 0	16.8	−0.008
26.639	334.35	2 1 0	50.1	0.015	48.592	187.21	0 3 2	5.0	−0.008
27.390	325.35	0 0 2	93.4	−0.006	49.686	183.34	0 2 3	14.3	−0.020
28.438	313.59	1 2 0	5.6	0.029	50.108	181.90	2 1 3	37.3	−0.020
29.381	303.74	0 2 1	23.5	0.003			1 2 3		0.007
30.028	297.34	2 1 1	100.0	0.007	52.795	173.25	3 2 2	2.9	−0.011
31.656	282.41	1 2 1	3.2	0.014	54.528	168.15	2 3 2	11.9	−0.008
32.579	274.62	1 1 2	12.2	0.014	54.936	167.00	4 2 0	4.7	−0.031
35.071	255.65	2 2 0	8.6	0.018	55.271	166.06	0 4 1	4.0	0.016
36.196	247.96	2 0 2	10.4	0.016	55.500	165.43	2 2 3	10.1	0.018
37.861	237.43	3 0 1	16.7	0.001	56.529	162.66	0 0 4	4.1	−0.018
38.072	236.16	0 2 2	16.5	−0.008	56.818	161.90	4 2 1	4.1	0.026
38.577	233.19	2 1 2	18.1	0.008	62.448	148.59	4 2 2	4.3	−0.021
39.908	225.72	1 2 2	5.2	0.003	69.959	134.36	0 5 1	3.1	0.022

[a] Cu $K\alpha_1$ radiation.
[b] $\Delta 2\theta = 2\theta_{ber} - 2\theta_{gem}$.

TABLE 3. X-ray-powder data of the high temperature form of $Ag_4P_2S_7$

$2\theta_{exp}$[a] (deg)	d_{exp} (pm)	h k l	I/I_0	$\Delta 2\theta$[b] (deg)	$2\theta_{exp}$[a] (deg)	d_{exp} (pm)	h k l	I/I_0	$\Delta 2\theta$[b] (deg)
11.371	777.57	1 0 0	16.1	−0.020	37.847	237.52	1 2 2	32.4	0.007
16.079	550.78	0 2 0	11.9	−0.009	39.051	230.47	2 3 1	6.7	0.020
17.793	498.11	1 1 1	15.0	−0.017			3 0 2		
19.714	449.98	1 2 0	29.3	0.004	41.923	215.33	2 0 2	54.7	0.010
22.826	389.28	2 0 0	18.1	−0.012	43.602	207.41	0 5 1	10.7	−0.016
24.945	356.68	2 1 1	59.5	0.015	44.119	205.10	0 4 2	11.3	−0.005
28.018	318.21	2 2 0	100.0	0.014	45.011	201.24	2 1 3	42.3	−0.019
29.047	307.17	0 0 2	79.2	−0.003	47.743	190.35	1 4 2	18.1	0.009
30.211	295.59	2 0 1	29.3	−0.012	50.448	180.76	1 5 2	24.7	0.020
31.300	285.55	2 1 1	55.1	−0.007	51.227	178.19	4 2 2	11.6	−0.013
31.993	279.53	2 0 2	16.5	0.001	51.669	176.77	3 0 2	18.0	0.008
32.695	273.68	1 2 2	32.7	−0.011			2 5 1		
33.364	268.34	0 2 2	34.9	0.002			3 4 2		
34.481	259.90	1 4 0	39.9	0.018	51.924	175.95	0 6 1	23.0	−0.013
34.711	258.23	3 1 1	25.1	0.020					

[a] Cu $K\alpha_1$ radiation.
[b] $\Delta 2\theta = 2\theta_{ber} - 2\theta_{gem}$.

TABLE 4. X-ray powder data of $(CuPS_3)_n$[a]

$2\theta_{exp}$[b] (deg)	d_{exp} (pm)	I/I_0		$2\theta_{exp}$[b] (deg)	d_{exp} (pm)	I/I_0	
11.724	754.18	19.8	$(CuPS_3)_n$	50.169	181.69	27.7	$(CuPS_3)_n + Cu_3PS_4$
17.836	496.88	22.6	$(CuPS_3)_n$	53.723	170.48	80.9	$(CuPS_3)_n + Cu_3PS_4$
26.697	333.64	23.8	$(CuPS_3)_n$	54.664	167.76	3.1	$(CuPS_3)_n$
28.257	315.57	100.0	$(CuPS_3)_n + Cu_3PS_4$	56.646	162.35	6.5	$(CuPS_3)_n$
29.359	303.97	51.9	Cu_3PS_4	58.325	158.07	5.8	$(CuPS_3)_n$
29.877	298.81	35.4	$(CuPS_3)_n$	58.442	157.79	17.1	$(CuPS_3)_n + Cu_3PS_4$
30.767	290.37	3.1	$(CuPS_3)_n + Cu_3PS_4$	59.037	156.34	20.2	$(CuPS_3)_n + Cu_3PS_4$
31.940	279.97	54.5	$(CuPS_3)_n + Cu_3PS_4$	59.238	155.86	7.3	$(CuPS_3)_n + Cu_3PS_4$
33.861	264.51	20.5	$(CuPS_3)_n$	60.598	152.68	9.3	$(CuPS_3)_n + Cu_3PS_4$
34.989	256.23	4.9	$(CuPS_3)_n + Cu_3PS_4$	60.957	151.86	6.4	$(CuPS_3)_n + Cu_3PS_4$
36.185	248.03	7.3	$(CuPS_3)_n$	66.858	139.82	4.1	$(CuPS_3)_n + Cu_3PS_4$
41.231	218.77	21.1	$(CuPS_3)_n + Cu_3PS_4$	67.107	139.36	3.4	$(CuPS_3)_n$
41.918	215.34	4.1	$(CuPS_3)_n$	71.363	132.06	2.7	$(CuPS_3)_n$
46.558	194.91	3.2	$(CuPS_3)_n$	71.901	131.20	3.1	$(CuPS_3)_n$
48.951	185.92	11.7	$(CuPS_3)_n$	75.817	125.37	2.9	$(CuPS_3)_n$
49.132	185.28	4.2	$(CuPS_3)_n$	76.464	124.47	8.0	$(CuPS_3)_n + Cu_3PS_4$
49.924	182.52	28.1	$(CuPS_3)_n + Cu_3PS_4$				

[a] Samples were always contaminated by traces of Cu_3PS_4.
[b] Cu $K\alpha_1$ radiation.

TABLE 5. Compounds of the systems Tl_2S–P_4S_{10} and Sb_2S_3–P_4S_{10}

Compound	Type	T_m (K)	Space group	Lattice parameters (pm)	Reference
Tl_3PS_4	Congruent	812	*Pnma*	$a = 872.1(5)$, $b = 1085.4(0)$, $c = 895.11$	
				$a = 873.3(5)$, $b = 1084.9(6)$, $c = 895.9(5)$[a]	16
$Tl_2P_2S_6$	Congruent	842	*Immm*	$a = 789.04$, $b = 689.51$, $c = 905.46$	
				$a = 793.2(4)$, $b = 689.2(4)$, $c = 901.9(5)$[a]	17
$SbPS_4$	Congruent	854		$a = 1306.3(5)$, $c = 627.9(5)$	
				$a = 1303$, $c = 525$	19

[a] Single crystal data.

Acknowledgments

We wish to thank the Deutsche Forschungsgemeinschaft (SFB 225: Oxidische Kristalle), Professor Dr. H. Haeuseler (Universität Siegen) for the measurement of the spectra, and the Fonds der Chemischen Industrie for financial support.

References

1 L. Bohaty, personal communication, 1990.
2 B. Gather, *Ph.D. Thesis*, T.U. Clausthal, 1973.
3 H. T. Evans, D. E. Appleman and D. S. Handwerker, LSUCRE-Program Am. Cryst. Ass., Cambridge, MA, 1963, Program 42.
4 W. F. Kuhs, M. Schulte-Kellinghaus, V. Krämer and R. Nitsche, *Z. Naturforsch., 32b* (1977) 1100.
5 J. Garin and E. Parthe, *Acta Crystallogr., B 28* (1972) 3672.
6 R. Nitsche and P. Wild, *Mater. Res. Bull., 5* (1970) 491.
7 W. F. Kuhs, R. Nitsche and K. Scheunemann, *Mater. Res. Bull., 14* (1979) 241.
8 R. Blachnik and U. Wickel, *Z. Naturforsch., 35b* (1980) 1268.
9 P. Toffoli, P. Khodadad and N. Rodier, *Acta Crystallogr., B38* (1982) 2374.
10 P. Toffoli, P. Khodadad and N. Rodier, *Acta Crystallogr., B33* (1977) 1492.
11 P. Toffoli, P. Khodadad and N. Rodier, *Acta Crystallogr., B 34* (1978) 3561.
12 U. Pätzmann and W. Brockner, *Z. Naturforsch., 38a* (1983) 27.
13 L. Pauling and S. Weinbaum, *Z. Kristallogr., 88* (1934) 48.
14 K. Yvon, W. Jeitschko and E. Parthe, *J. Appl. Crystallogr., 10* (1977) 73.
15 A. I. Soklakov and V. V. Nechaeva, *Inorg. Mater., 6* (1970) 873.
16 P. Toffoli, P. Khodadad and N. Rodier, *Bull. Soc. Chim. Fr.*, (1981) 429.
17 C. Wibbelmann, W. Brockner, B. Eisenmann and H. Schäfer, *Z. Naturforsch., 38b* (1983) 1575.
18 V. J. Tkachenko, L. G. Novikova and Ju. V. Voroshilova, *Russ. J. Phys. Chem., 64* (1990) 482.
19 V. S. D'ordyai, I. V. Galagovets, E. Yu. Peresh, Yu. V. Voroshilov, V. S. Gersimenko and V. Yu. Slivka, *Russ. J. Inorg. Chem., 24* (1979) 1603.
A. I. Soklakov and V. V. Nechaeva, *Izv. Akad. Nauk SSSR, Neorg. Mater., 5* (1969) 989.
20 M. Queignec, M. Evain, R. Brec and C. Sourisseau, *J. Solid State Chem., 63* (1986) 89.
21 O. Sala and M. L. A. Temperini, *Chem. Phys. Lett., 36* (1975) 652.
22 M. L. A. Temperini, O. Sala and H. J. Bernstein, *Chem. Phys. Lett., 59* (1978) 10.